Direct Dynamic Studies on Tropospheric Reactivity of Fluorinated Ethanes: Scope and Limitations of the General Reaction Parameter Method

S. Sekušak* and A. Sabljić

Ruđer Bošković Institute, Department of Physical Chemistry, P.O. Box 180,
HR-10002 Zagreb, Republic of Croatia

Received: August 4, 2000; In Final Form: December 7, 2000

A direct dynamics study on the gas-phase reactions of OH radical with polyfluorinated ethanes has been carried out. Their thermal rate constants were calculated using canonical variational transition state theory augmented by multidimensional semiclassical small and large curvature tunneling approximations. The potential energy surface for the 1,1- and 1,2-difluoroethane reaction with hydroxyl radical was investigated with ab initio methods and a semiempirical PM3 Hamiltonian using specific reaction parameters (SRP). The reaction proceeds via hydrogen atom abstraction from both α and β carbon atoms with respect to fluorine substitution. In total, 26 stationary points were found, corresponding to the three and four reaction channels for 1,1- and 1,2-difluoroethane, respectively. Reactant molecules and product radicals, transition state structures, and pre-reactive complexes were characterized. Pre-reactive complexes are formed on both sides of the reaction path, directing the reaction to the different reaction channels. The main interactions between reactant and product molecules in the pre-reactive complexes are weak hydrogen bonds between hydrogen atoms from the OH radical or water, and fluorine atoms from the hydrocarbon moiety. Data obtained from the electronic structure calculations were further used to calculate the reaction rate coefficients. Variational transition state theory was used for that purpose in terms of the interpolated and direct versions. Good agreement is obtained with experimental data, and measured rate coefficients are reproduced within a factor of 2. Reaction rate constants for tri-, tetra-, and penta-fluorinated ethanes were calculated in terms of direct dynamics using SRP derived for the ethane reaction with the OH radical to explore the scope and limitations of SRP as a general reaction parameter set.

Introduction

Reactions of hydroxyl (OH) radical with halogenated ethanes are of particular interest in atmospheric and combustion chemistry.[1] This reaction is the rate-determining step in the tropospheric degradation of hydrohalocarbons.[2] During the past decade hydrofluorocarbons have replaced chlorofluorocarbons in many applications because of their lower potential to deplete ozone.[3]

This paper is a continuation of our long-term research efforts[4] to investigate the potential energy surfaces and reaction dynamics of OH radical reactions with hydrocarbons and their halogenated derivatives as well as to develop an affordable and reliable methodology for calculating the reaction rate constants of large molecular systems. Such methodology will enable efficient evaluation of the tropospheric fate, the ozone depletion potential, and the global warming potential of existing and future hydrohalocarbon products. Our early studies were focused on the detailed analysis of structural and energetic characteristics of reactants, products, and transition state structures of OH radical reactions with model compounds ethane,[4a] fluoroethane,[4b] and chloroethane.[4a] Studies on methane,[5] halogenated methanes,[6] ethane,[7] halogenated ethanes,[8] and propane[9] were performed by several other research groups.

More recently, the detailed studies of the ethane,[4c] fluoroethane,[4c] and chloroethane[4c] reactions with OH radical were

undertaken in terms of direct and interpolated reaction-path dynamics.[10–12] The contribution from tunneling effect was evaluated using the semiclassical zero-curvature and small-curvature tunneling approximations.[10,13] This approach has been used to calculate the reaction rate constants for temperatures from 200 to 1000 K. The calculated thermal reaction rate constants agreed well with the experimental results.

In addition, the semiempirical PM3 Hamiltonian was reparametrized to specifically describe the reaction of ethane with OH radical using the critical parts of potential energy surfaces calculated by ab initio methods with a correlated wavefunction.[4d] In this way, a set of specific reaction parameters (SRP) was obtained that enabled us to carry out direct dynamic calculations with multidimensional tunneling calculations with large curvature approximations.[10,14] Furthermore, the reaction rate constants for fluoroethane,[4d] chloroethane,[4d] and a set of larger hydrocarbons[4d] were calculated using derived SRP parameters to test their applicability in direct dynamic calculations of the reaction rate constants. A good agreement of the SRP rate constants with the experimental and ab initio rate constants was achieved, showing that the SRP constants can be used as general reaction parameters (GRP) capable of yielding quantitatively correct rates when applied to analogous reaction mechanisms.

The main objectives of this paper are to investigate the potential energy surfaces of the OH radical reactions with 1,1- and 1,2-difluoroethane, i.e., the model compounds for polyfluorinated alkanes, and to explore the scope and limitations of

---

* Corresponding author. E-mail: sekusak@rudjer.irb.hr. Fax: +385–1–468–0245.

Tropospheric Reactivity of Fluorinated Ethanes

J. Phys. Chem. A, Vol. 105, No. 10, 2001 **1969**

the specific reaction parameters in direct dynamic calculations of their reaction rate constants. Thus, the potential energy surface was fully characterized for the OH radical reactions with both difluoroethanes using ab initio methods with a correlated wavefunction to evaluate the effect of fluorine substitution on the energetics and kinetics of these reactions.

$$CHF_2CH_3 + \cdot OH \rightarrow \cdot CF_2CH_3 + H_2O \qquad (R1a)$$

$$CHF_2CH_3 + \cdot OH \rightarrow CHF_2CH_2 \cdot + H_2O \qquad (R1b)$$

$$CH_2FCH_2F + \cdot OH \rightarrow CH_2FCHF \cdot + H_2O \qquad (R2)$$

Data obtained from electronic structure calculations were then used to correct the potential energy surface obtained by the semiempirical PM3-SRP Hamiltonian. Finally, the applicability of the SRP parameters was tested on the OH radical reactions with the complete set of tri-, tetra-, and penta-fluorinated ethanes. Their reaction rate constants were calculated in terms of direct dynamics based on the SRP potential energy surface with multidimensional semiclassical small and large tunneling corrections. Results are compared with the experimental reaction rates.

Methods

Electronic Structure Calculations. Potential energy surfaces for reactions R1 and R2 were scanned, using second-order Moller Plesset perturbation theory (MP2) relative to a UHF reference,[15] in order to find and characterize the following stationary points: reactants, products, transition states and van der Waals complexes formed on the reactant and product side of the minimum energy path (MEP). It was already shown that electron correlation plays an important role in describing H-abstraction reactions.[4−9] DFT methods, both in their pure or hybrid forms failed to correctly describe weak H−F interactions that govern the formation of the transition-state structures and van der Waals complexes of the OH radical reaction with haloethanes.[16] A split valence basis set of a triple-ζ quality with one set of diffuse and two sets of polarization functions on the heavy atoms and one set of polarization functions on the hydrogen atoms, 6-311+G(2d,p),[17] was used in the optimization procedure and for the calculation of the force constants. We will call this basis set *bs1*. Reaction energetics were further improved by adding additional sets of polarization functions on all atoms and a set of diffuse functions on the hydrogen atom, resulting in the 6-311++G(3df,2pd) basis set.[17,18] That we will call *bs2*. It was already shown that the MP2/6-311++G-(3df,2pd) energetics was very similar to the one calculated at G2 level for ethane, fluoroethane, and chloroethane reactions with OH radical.[16] Therefore, we expect to achieve the same accuracy for difluoroethanes.

For the open-shell systems, Schlegel's spin projection scheme was used to eliminate spin contamination arising from states with spin (s+1) to (s+4).[19]

All energies were zero-point corrected. For reaction enthalpies, thermal energies at 298 K were added. All calculations were carried out with the *Gaussian94* program package.[20] The NBO analysis was performed with the *NBO program* (version 3.1),[21] which is integrated into the *Gaussian94* suite of programs. The NBO method is discussed in detail elsewhere.[21]

Ab initio data were used to calculate reaction rate coefficients in terms of variational transition state theory and for validation and improvement of the PM3-SRP potential energy surface

generated by the specific reaction parameters obtained previously for the ethane reaction with OH radical.[4d]

Reaction Rate Calculations. Direct dynamics, within the dual-level dynamics scheme,[22] was applied in this work. The potential energy surface necessary for the dynamics calculations was evaluated "on the fly"; i.e., dynamical quantities were calculated using the semiempirical electronic structure calculations for all required energies, forces, and Hessians, without a need for an analytic potential energy function.[11,23,24]

The reaction path was computed using an Euler integrator[25] with a gradient step-size of 0.01 a_0, and the Hessian was recalculated every 9 steps.[26] The semiempirical SRP surface was further improved using the ab initio data by means of interpolated corrections (IC).[27] The geometries and vibrational frequencies were corrected with those calculated at the MP2-(full)/6-311+G(2d,p) level, and the energetics were further improved using the MP2(full)/ 6-311++G(3df,2pd) results. The vibrational frequencies were corrected using the interpolated-corrections-based-on-arithmetic-differences scheme (ICA).[28] The energy along the reaction path, $V_{MEP}(s)$, was improved by fitting the ab initio results for the reactants, products, and saddle point to an Eckart function.[22a]

Tunneling was included through the microcanonical optimized multidimensional (μOMT),[29] large-curvature (LCT),[10,14] and small-curvature (SCT)[10,13] tunneling approximations. The exit channel for the large-curvature tunneling was restricted to the vibrational ground state. Tunneling into excited states was investigated and was found to make a negligible contribution.[4d]

The low frequency modes that become imaginary along the reaction path due to the use of rectilinear coordinates were interpolated directly from the frequencies of the transition state, reactant, and product structures in terms of the IVTST-0 treatment.[26a]

According to the standard notation of dual-level dynamics,[21b] the notation for IVTST-IC and direct dynamics rate constants are given as MP2(full)/bs2//PM3-SRP. Throughout the rest of this paper we will use a shorthand notation; i.e., MP2/bs2//SRP. When tunneling corrections are included, the label (MP2/bs2//SRP)/μOMT will be used.

The dynamic calculations were carried out using the *POLYRATE* (version 7.8.1)[28] and *MORATE* (version 7.5) programs.[30]

Experimental Data

Experimental data for studied reactions are taken from Atkinson's compilation on the gas-phase tropospheric chemistry of organic compounds.[1] There is a number of experimental rate coefficients for 1,1-difluoroethane, but only in a narrow temperature region from 200 to 400 K. Furthermore, an experimental rate coefficient for 1,2-difluoroethane is available only at 298 K. Experimental activation energies for 1,1-difluoroethane (2.1±0.3, and 1.9±0.5 kcal mol^{-1}) were calculated from the temperature dependence of the rate coefficients. Experimental reaction enthalpy for the reaction R1a, calculated from the experimental heats of formation of reactants and products,[20] is −20.7 kcal mol^{-1}. To the best of our knowledge, there are no experimental reaction enthalpies published for reactions R1b and R2.

Results and Discussion

Reaction charts with the possible reaction channels and schematic presentation of all stationary points found for the reactions R1 and R2 are shown in Schemes 1 and 2. Reaction flow is analogous to the reactions of monohalogenated ethanes
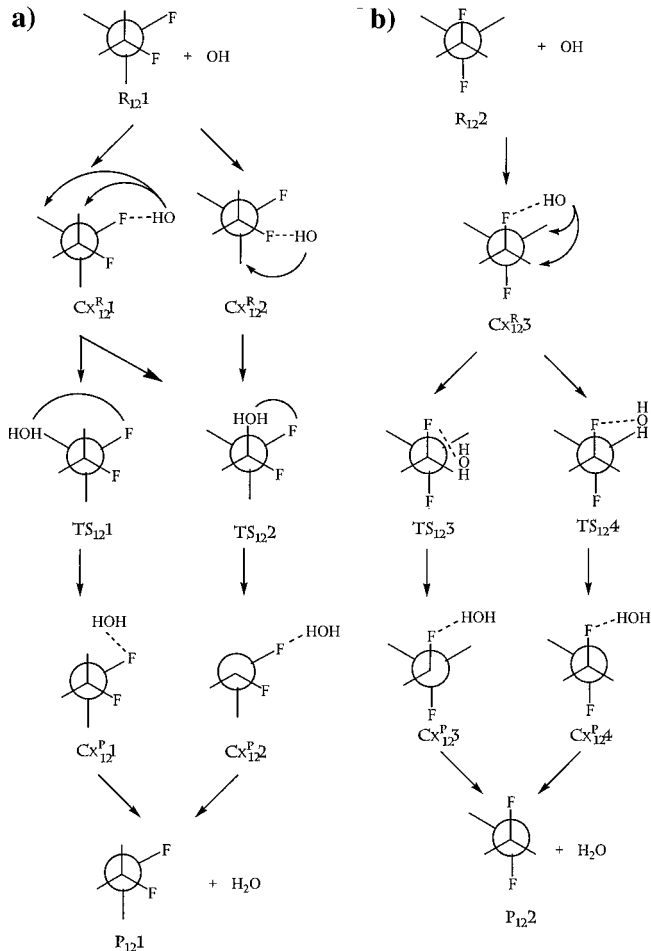
SCHEME 1.   Reaction Chart for 1,1-Difluoroethane Reaction with OH Radical

SCHEME 2.   Reaction Chart for 1,2-Difluoroethane Reaction with OH Radical
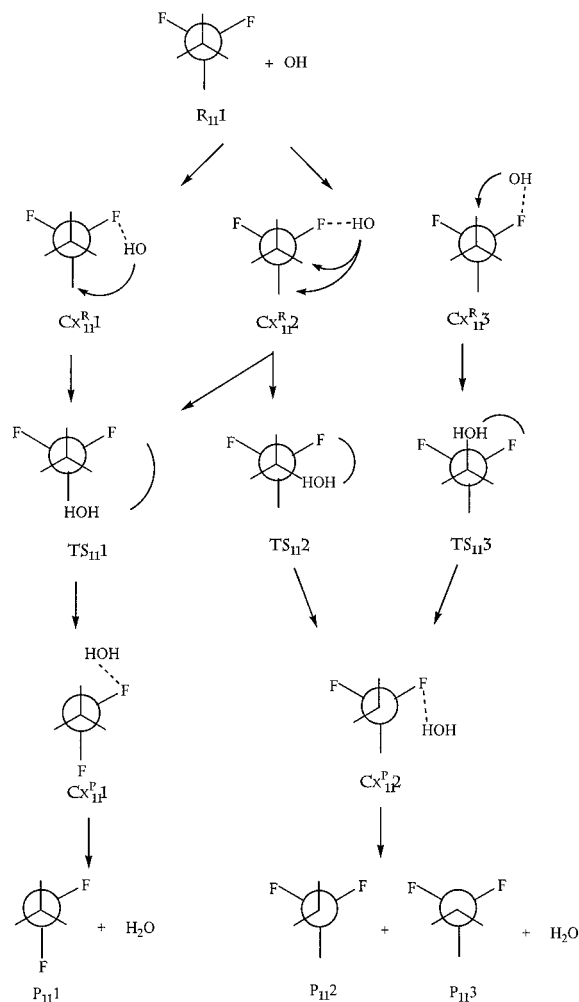
with OH radicals,[4,32] showing that reactions proceed via an indirect mechanism. As a first step in the reactions, hydrogen-bonded complexes (Cx^R) are formed. They are characterized by an attractive interaction between fluorine and hydrogen atom of the OH radical. As the reaction proceeds further from Cx^R to the transition-state structures, the OH radical rotates around the H-bond approaching the abstracting hydrogen. Further, in the course of the reaction the reactive C−H bond is broken and a water molecule is formed. Again, a van der Waals complex is formed, this time between the products of the reaction (Cx^P). The final stage is the dissociation of the Cx^P into products.

Equilibrium geometries and vibration frequencies of reactants and products, transition-state structures, and reactive complexes are described in more detail in section 1. In section 2 complete energetics is given, and in section 3 properties of the SRP potential energy surfaces are discussed. In section 4 the results of the reaction rate calculations are presented.

1. Optimized Structures and Vibration Frequencies. *A. Reactants and Products.* Geometrical parameters for the equilibrium structures of reactants and products of reactions R1 and R2 are given in Table 1 together with available experimental values. 1,1-Difluoroethane has only one stable conformation of C_s symmetry, whereas 1,2-difluoroethane has two conformers: gauche and anti. The zero-point corrected energy difference between the two conformers of 0.87 kcal mol^{-1} supports experimental data obtained from the gas-phase Raman spec-
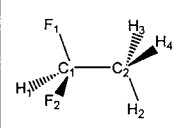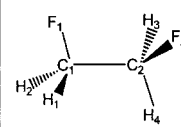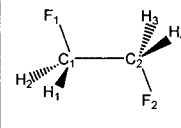
trum[33] (0.81 kcal mol^{-1}), electron diffraction[33] (0.93 kcal mol^{-1}), NMR experiments[33] (0.60 and 0.83), and previous ab initio calculations at the MP4/6-311++G(d,p) level[33] (0.70 kcal mol^{-1}). The peculiar stability of the gauche conformer, the so-called "gauche effect", has been explained as a consequence of the nodal structure of the singly occupied orbital in the CFH$_2$ radical.[34]

Good agreement with experimental data[35] is obtained for both 1,1- and 1,2-difluoroethane geometries. The root-mean-square (rms) error for the bond lengths is 0.006 Å, and for the angles 1.1°. A noticeable difference is obtained for the $\theta(H_1C_1C_2)$ angle. However, the experimental value is given only as a mean of all CCH angles in the molecule. The carbon−carbon bond length is practically identical for 1,1-difluoroethane and gauche conformer of 1,2-difluoroethane. In the anti conformer, the C−C bond length is elongated for 0.112 Å in agreement with its lesser stability.

Three different radicals can be formed as products of reaction R1. Radical P$_{11}$1 is formed by α-abstraction, and radicals P$_{11}$2 and P$_{11}$3 by β-abstraction. The last two radicals are actually two different conformers very close in energy ($\Delta E = 0.2$ kcal mol^{-1} at the MP2/bs2 level); therefore, only the more stable P$_{11}$2 is taken into account in further discussion. Two radical products are formed in the R2 reaction; P$_{12}$1 is formed by H-abstraction from the gauche conformer and P$_{12}$2 by H-abstraction from the anti conformer of 1,2-difluoroethane. C−C and C−F bond lengths are shorter for all radical species with respect to the parent difluorocarbon molecules as a result of

Tropospheric Reactivity of Fluorinated Ethanes

J. Phys. Chem. A, Vol. 105, No. 10, 2001 **1971**

TABLE 1: Calculated and Experimental Geometries for (a) Reactants and (b) Product Radicals in OH Radical Reaction with 1,1- and 1,2-Difluoroethane

a)

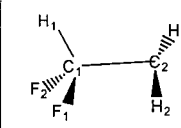| Compound	Parameter	Calc.[a]	Exp.	
OH	r(O-H)	0.971	0.971[b]	
H$_2$O	r(O-H)	0.963	0.958[b]	
	θ(HOH)	104.7	104.5	
R$_{11}$1 (C$_s$)	r(C$_1$-C$_2$)	1.498	1.498[f,g]	
	r(C$_1$-F$_1$)= r(C$_1$-F$_2$)	1.371	1.364	
	r(C$_1$-H$_1$)	1.091	1.081	
	r(C$_2$-H$_2$)= r(C$_2$-H$_3$)= r(C$_2$-H$_4$)	1.090	1.081	
	θ(F$_1$C$_1$C$_2$)= θ(F$_2$C$_1$C$_2$)	110.0	110.6	
	θ(H$_1$C$_1$C$_2$)	114.7	110.1	
	θ(H$_2$C$_2$C$_1$)	109.0	110.1	
	θ(H$_3$C$_2$C$_1$)= θ(H$_4$C$_2$C$_1$)	109.7	110.1	
	θ(F$_1$C$_1$F$_2$)	107.0	107.4	
	θ(F$_1$C$_1$H$_1$)= θ(F$_2$C$_1$H$_1$)	107.4	108.5	
	θ(H$_2$C$_2$H$_3$)=θ(H$_2$C$_2$H$_4$)=θ(H$_3$C$_2$H$_4$)	109.5	107.0	
	τ (FCCF)	117.7	118.9	
R$_{12}$1 (C$_2$)	r(C$_1$-C$_2$)	1.499	1.493[c]	1.503[d]
	r(C$_1$-F$_1$)= R(C$_2$-F$_2$)	1.392	1.390	1.389
	r(C$_1$-H$_1$)= R(C$_2$-H$_3$)	1.091	1.099	1.103
	r(C$_1$-H$_2$)= R(C$_2$-H$_4$)	1.093	1.093	1.103
	θ(F$_1$C$_1$C$_2$)= θ(F$_2$C$_2$C$_1$)	110.2	110.6	110.3
	θ (H$_1$C$_1$C$_2$)= θ(H$_3$C$_2$C$_1$)	110.7	108.4	110.0
	θ (H$_2$C$_1$C$_2$)= θ(H$_4$C$_2$C$_1$)	109.8	111.3	110.0
	θ (F$_1$C$_1$H$_1$)= θ(F$_2$C$_2$H$_3$)	108.0	109.6	109.0
	θ (F$_1$C$_1$H$_2$)= θ(F$_2$C$_2$H$_4$)	108.1	107.8	109.0
	θ (H$_1$C$_1$H$_2$)= θ(H$_3$C$_2$H$_4$)	110.0	109.1	108.5
	τ (FCCF)	70.5	71.0	71.3
R$_{12}$2 (C$_{2h}$)	r(C$_1$-C$_2$)	1.511	1.506[e]	
	r(C$_1$-F$_1$)= R(C$_2$-F$_2$)	1.394	1.400	
	r(C$_1$-H$_1$) = R(C$_2$-H$_3$)= r(C$_1$-H$_2$)= R(C$_2$-H$_4$)	1.090	1.092	
	θ(F$_1$C$_1$C$_2$)= θ(F$_2$C$_2$C$_1$)	107.8	107.3	
	θ (H$_1$C$_1$C$_2$)= θ(H$_3$C$_2$C$_1$)= θ (H$_2$C$_2$C$_2$)=θ(H$_4$C$_2$C$_1$)=	111.1	111.6	
	θ (F$_1$C$_1$H$_1$)= θ(F$_2$C$_2$H$_3$)= θ (F$_1$C$_1$H$_2$)= θ(F$_2$C$_2$H$_4$)	108.5	107.8	
	θ (H$_1$C$_1$H$_2$)= θ(H$_3$C$_2$H$_4$)	109.9	110.7	
	τ (FCCF)	180.0	180.0	

a - UMP2/6-311+G(2d,p)
b - Ref 34a
c - Ref. 34b
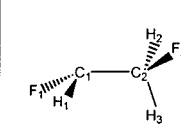d - Ref. 34c
e - Ref. 34d
f - Ref. 34e
g - C-H mean, ∠CCH(mean)
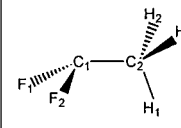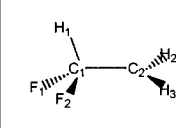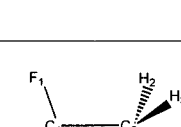
b)

Compound	Parameter	Calc.
P$_{11}$1 (C$_s$)	r(C$_1$-C$_2$)	1.485
	r(C$_1$-F$_1$)=r(C$_1$-F$_2$)	1.340
	r(C$_2$-H$_1$)	1.095
	r(C$_2$-H$_2$)=r(C$_2$-H$_3$)	1.088
	θ(F$_1$C$_1$C$_2$)=θ(F$_2$C$_1$C$_2$)	114.9
	θ(H$_1$C$_2$C$_1$)	109.9
	θ(H$_2$C$_2$C$_1$)=θ(H$_3$C$_2$C$_1$)	109.1
	θ(F$_1$C$_1$F$_2$)	109.5
	θ(H$_1$C$_2$H$_2$)=θ(H$_1$C$_2$H$_3$)	109.1
	τ (F$_2$C$_1$C$_2$H$_2$)	175.9
P$_{11}$2 (C$_1$)	r(C$_1$-C$_2$)	1.475
	r(C$_1$-F$_1$)	1.368
	r(C$_1$-F$_2$)	1.381
	r(C$_1$-H$_1$)	1.090
	r(C$_2$-H$_2$)	1.079
	r(C$_2$-H$_3$)	1.079
	θ(F$_1$C$_1$C$_2$)	110.1
	θ(F$_2$C$_1$C$_2$)	110.6
	θ(H$_1$C$_1$C$_2$)	114.4
	θ(H$_2$C$_2$C$_1$)	118.9
	θ(H$_3$C$_2$C$_1$)	119.7
	τ (H$_1$C$_1$C$_2$H$_2$)	154.0
P$_{11}$3 (C$_s$)	r(C$_1$-C$_2$)	1.477
	r(C$_1$-F$_1$)=r(C$_1$-F$_2$)	1.371
	r(C$_1$-H$_1$)	1.094
	r(C$_2$-H$_2$)=r(C$_2$-H$_3$)	1.078
	θ(F$_1$C$_1$C$_2$)=θ(F$_2$C$_1$C$_2$)	110.2
	θ(H$_1$C$_2$C$_1$)	114.7
	θ(H$_2$C$_2$C$_1$)=θ(H$_3$C$_2$C$_1$)	119.2
	θ(F$_1$C$_1$F$_2$)	107.7
	θ(H$_2$C$_2$H$_3$)	120.8
	τ (F$_2$C$_1$C$_2$H$_2$)	154.1
P$_{12}$1 (C$_1$)	r(C$_1$-C$_2$)	1.469
	r(C$_1$-F$_1$)	1.343
	r(C$_2$-F$_2$)	1.411
	r(C$_1$-H$_1$)	1.081
	r(C$_2$-H$_2$)	1.090
	r(C$_2$-H$_3$)	1.090
	θ(F$_1$C$_1$C$_2$)	116.1
	θ(F$_2$C$_2$C$_1$)	107.3
	θ(H$_1$C$_1$C$_2$)	124.3
	θ(H$_2$C$_2$C$_1$)	110.1
	θ(H$_3$C$_2$C$_1$)	110.8
	θ(F$_1$C$_1$H$_1$)	113.6
	θ(F$_2$C$_2$H$_2$)	107.0
	θ(F$_2$C$_2$H$_3$)	107.2
	τ (FCCF)	77.5
P$_{12}$2 (C$_1$)	r(C$_1$-C$_2$)	1.486
	r(C$_1$-F$_1$)	1.350
	r(C$_2$-F$_2$)	1.391
	r(C$_1$-H$_1$)	1.083
	r(C$_2$-H$_2$)	1.092
	r(C$_2$-H$_3$)	1.096
	θ(F$_1$C$_1$C$_2$)	113.3
	θ(F$_2$C$_2$C$_1$)	108.3
	θ(H$_1$C$_1$C$_2$)	122.1
	θ(H$_2$C$_2$C$_1$)	112.0
	θ(H$_3$C$_2$C$_1$)	110.7
	θ(F$_1$C$_1$H$_1$)	114.0
	θ(F$_2$C$_2$H$_2$)	107.8
	θ(F$_2$C$_2$H$_3$)	109.0
	τ (FCCF)	174.1

the electron density redistribution and larger polarization of the C−F and C−C bonds.

Vibrational frequencies for the 1,1-difluoroethane[36] and 1,2-difluoroethane[37] have already been published at a similar level of theory, but here complete assignation for the reactant and product species is given for the sake of completeness (Table 2).

The computed harmonic vibration frequencies are generally overestimated, stretching modes having the largest deviations. Root-mean-square (rms) values are 76 and 84 cm^{-1} for 1,2- and 1,1-difluoroethane, respectively. Deviations are halved (35 and 47 cm^{-1}) if the scaling factor of 0.9748 is used.[38] It should be noted that this scaling factor is derived for the MP2/6-311G-(d,p) level of theory, and the same scaling factor is used for stretching and bending modes.

Experimental vibration frequencies are not available for the product radicals. Therefore, we hope that computed frequencies and their assignation will be helpful in experimental identification of these radical species. Results are given in Table 3.

B. Transition-State Structures. Three transition-state structures were found for the 1,1-difluoroethane reaction with OH radical. One reaction channel was found for the abstraction from the α-carbon atom (R1a reaction) and two for the abstraction from the β-carbon atom (R1b reaction). Four reactive channels were found for reaction R2; two for gauche and two for anti rotamer reaction with OH radical. Selected geometrical parameters are

TABLE 2: Comparison of Observed and Calculated Vibration Frequencies (cm^{-1}) for the 1,1-Difluoroethane and Gauche and Anti Conformers of 1,2-Difluoroethane

1,1-Difluoroethane Conformers

symm	no.	vibration[a]	calc.[b]	exp[c,d]
A′	ν_1	$\nu(CH_3)_a$	3193	3016, 3015
A′	ν_2	$\nu(CH_3)_s$	3136	2975, 2975
A′	ν_3	$\nu(CH_3)_s$	3093	2959, 2964
A′	ν_4	$\delta(CH_2)$	1514	1466, 1457
A′	ν_5	$\omega(CH_3)-\omega(CH)$	1409	1413, 1413
A′	ν_6	$\omega(CH_3)+\omega(CH)$	1459	1362, 1357
A′	ν_7	$\delta(CH), \nu(CF)_s$	1171	1171, 1171
A′	ν_8	$\nu(CC), \rho(CH_3), \nu(CF)_a$	1155	1142, 1140
A′	ν_9	$\nu(CF)_s, \delta(CH), \nu(CC)$	881	868, 868
A′	ν_{10}	$\delta(CF_2)+\delta(CH_3)$	566	569, 569
A′	ν_{11}	$\delta(CF_2)-\delta(CH_3)$	464	469, 468
A″	ν_{12}	$\nu(CH_3)_a$	3190	3015
A″	ν_{13}	$\delta(CH_2)$	1513	1457
A″	ν_{14}	$\delta(CH), \nu(CF)_s$	1402	1164, 1362
A″	ν_{15}	$\delta(CH), \nu(CF)_a$	1150	1149, 1135
A″	ν_{16}	$\tau(CH_2), \nu(CF)_a$	955	942, 942
A″	ν_{17}	$\tau(CH_2)$	383	383
A″	ν_{18}	torsion	241	222

Gauche and Anti Conformers

symm.[e]	no.	vibration[f]	gauche calc.[g]	gauche exp[h]	anti calc.[g]	anti exp[h,i]
A_g	ν_1	$\nu(CH_2)_s$	3099	2958	3109	2974
A_g	ν_2	$\delta(CH_2)_s$	1521	1460	1549	
A_g	ν_3	$\omega(CH_2)$	1461	1410	1465	
A_g	ν_4	$\nu(CF)_s$	1122	1079	1061	
A_g	ν_5	$\nu(CC)$	882	865	1112	974
A_g	ν_6	$\delta(CCF)_a$	326	327	278	457
A_u	ν_7	$\nu(CH_2)_a$	3158	2995	3190	
A_u	ν_8	$\tau(CH_2)$	1321	1284	1247	
A_u	ν_9	$\rho(CH_2)$	1145	1116	824	
A_u	ν_{10}	torsion	154	147	121	117, 145
B_g	ν_{11}	$\nu(CH_2)_a$	3169	3001	3167	
B_g	ν_{12}	$\tau(CH_2)$	1278	1244	1315	1087
B_g	ν_{13}	$\rho(CH_2)$	911	896	1187	1052
B_u	ν_{14}	$\nu(CH_2)_s$	3091	2985	3115	
B_u	ν_{15}	$\delta(CH_2)_a$	1520	1460	1555	
B_u	ν_{16}	$\omega(CH_2)$	1421	1377	1378	
B_u	ν_{17}	$\nu(CF)_a$	1090	1076	1069	1048
B_u	ν_{18}	$\delta(CCF)_s$	500	500	459	285

^{a} ν-stretch; δ-bend; ρ-rock; ω-wagging; τ-twist. ^{b} Calculated at MP2/6-311+G(2d,p) level. ^{c} Reference 35a. ^{d} Reference 35b. ^{e} A_g and A_u blocks for the trans conformer reduce to the A block for the gauche conformer. B_g and B_u reduce to the B block. ^{f} ν-Stretch, δ-bend, ρ-rock, ω-wagging, τ-twist ^{g} Calculated at MP2/6-311+G(2d,p) level. ^{h} Reference 36a. ^{i} Reference 36b.

given in Figures 1 and 2 for the R1 and R2 reactions, respectively.

Among three transition-state structures found for reaction R1, TS$_{11}$1 is the most reactant-like, with reactive distances r_{CH} = 1.187 Å and r_{OH} = 1.328 Å. The other two TS structures are different rotamers of the abstraction from the β-carbon atom. Reactive distances are r_{CH} = 1.204 Å and r_{OH} = 1.292 Å for the TS$_{11}$2 and r_{CH} = 1.208 Å and r_{OH} = 1.285 Å for the TS$_{11}$3. Calculated imaginary frequencies (see Figure 1) support the conclusion that TS$_{11}$1 is the earliest transition-state structure. The angle between carbon, hydrogen, and oxygen atoms (θ-(CHO)) is identical for all three TS structures, i.e., 163°.

The strongest intramolecular hydrogen bond is formed in TS$_{11}$3, r(HF) = 2.461 Å. Other two distances are r(HF) = 2.515 Å for TS$_{11}$2, and r(HF) = 2.875 Å for TS$_{11}$1. This interaction causes the asymmetry in the C–F distances of 0.011 Å for TS$_{11}$3 and 0.006 Å for other two TSs. It should be noticed that shorter H-bonds are formed with the fluorine atom on the neighboring carbon atom ("1,2") than on the same carbon atom ("1,1"). The same was found for the fluoroethane reaction with OH radical as well.[4b] The presence of the weak hydrogen bonding can be seen from the shift in the value of the vibration frequency that corresponds to the hindered rotation of the OH radical about the O···H$_{ab}$ reactive distance. Calculated frequencies are 149, 249, and 198 cm^{-1} for TS$_{11}$1, TS$_{11}$2, and TS$_{11}$3, significantly higher than, for example, 57 cm^{-1} calculated for the ethane reaction with OH radical (note that smaller basis set was used in this case).[4c]

There are four reactive channels for the 1,2-difluoroethane reaction with OH radical. Correspondingly, four transition-state structures were found, two for the gauche, and two for the anti conformer. In both cases TS structures with "1,2" hydrogen bonds are more reactant-like than the TS structures with "1,1" H-bonds. This can be seen from the values of imaginary vibration frequencies as well; ν_i(TS$_{12}$2) = 2016 cm^{-1}, ν_i(TS$_{12}$4) = 2006 cm^{-1}, ν_i(TS$_{12}$1) = 1884 cm^{-1}, and ν_i(TS$_{12}$3) = 1952 cm^{-1}.

Furthermore, the "1,2" TSs have significantly shorter H···F distances (2.390 for TS$_{12}$2, and 2.414 for TS$_{12}$4) than the "1,1" TS (2.907 for TS$_{12}$1, and 2.703 for TS$_{12}$3). Consequently, the hindered rotation frequencies are shifted to the higher values; 288 and 270 cm^{-1} for TS$_{12}$2 and TS$_{12}$4, and 184 and 186 cm^{-1} for TS$_{12}$1 and TS$_{12}$3. Strong asymmetry in the C–F bond lengths is caused by partial abstraction of the hydrogen atom. "1,1"

TABLE 3: Calculated Vibration Frequencies (cm^{-1}) for the Product Radicals of 1,1-Difluoroethane and 1,2-Difluoroethane Reactions with OH Radical

		1,1-Difluoroethane							1,2-Difluoroethane			
		P$_{11}$1		P$_{11}$2			P$_{11}$3		P$_{12}$1		P$_{12}$2	
no.	symm	vibration[a]	calc.[b]	vibration	calc.[b]	symm	vibration	calc.[b]	vibration[c]	calc.[d]	vibration	calc.[d]
ν_1	A′	$\nu(CH_3)_a$	3166	$\nu(CH_2)_a$	3347	A′	$\nu(CH_2)_s$	3223	$\nu(CH)$	3258	$\nu(CH)$	3239
ν_2	A′	$\nu(CH_3)_s$	3068	$\nu(CH_2)_s$	3217	A′	$\nu(CH)$	3098	$\nu(CH_2)_a$	3181	$\nu(CH_2)_a$	3135
ν_3	A′	$\delta(CH_2)$	1505	$\nu(CH)$	3145	A′	$\delta(CH_2)+\delta(CH)$	1487	$\nu(CH_2)_s$	3114	$\nu(CH_2)_s$	3061
ν_4	A′	$\delta(CH_3)$	1441	$\delta(CH_2)+\delta(CH)$	1450	A′	$\delta(CH_2)-\delta(CH)$	1399	$\delta(CH_2)-\delta(CH)$	1519	$\delta(CH_2)$	1534
ν_5	A′	$\nu(CC)-\nu(CF)_s$	1286	$\delta(CH_2)-\delta(CH)$	1421	A′	$\nu(CC)-\nu(CF)_s$	1168	$\delta(CH_2)+\delta(CH)$	1454	$\omega(CH_2)-\omega(CH)$	1461
ν_6	A′	$\Gamma(CF_2)-\rho(CH_3)$	1113	$\delta(CH)$	1381	A′	$\nu(CC)+\nu(CF)_s$	995	$\omega(CH_2)$	1385	$\omega(CH_2)+\omega(CH)$	1342
ν_7	A′	$\nu(CC)+\nu(CF)_s$	872	$\nu(CC)$	1161	A′	$\delta(CF_2)-\Gamma(CH_2)$	641	$\tau(CH_2)$	1291	$\tau(CH_2)$	1247
ν_8	A′	$\delta(CF_2)$	547	$\nu(CF)_s-\rho(CH_2)$	1155	A′	$\delta(CF_2)+\Gamma(CH_2)$	489	$\nu(CF)_s+\nu(CC)$	1222	$\nu(CF(H))+\nu(CC)$	1178
ν_9	A′	$\Gamma(CF_2)+\delta(CH_3)$	467	$\nu(CF)_a$	1024	A′	$\Gamma(CH_2)$	421	$\nu(CC)+\tau(CH_2)$	1129	$\nu(CC)$	1124
ν_{10}	A″	$\nu(CH_2)_a$	3205	$\nu(CF)_s+\rho(CH_2)$	899	A″	$\nu(CH_2)_a$	3352	$\nu(CF)_a+\nu(CC)$	971	$\nu(CF(H_2))$	1077
ν_{11}	A″	$\delta(CH_2)$	1506	$\delta(CH_2)-\Gamma(CH_2)$	616	A″	$\delta(CH)$	1396	$\nu(CC)-\tau(CH_2)$	921	$\rho(CH_2)_s-\Gamma(CCH)$	1019
ν_{12}	A″	$\nu(CF)_a$	1237	$\delta(CF_2)+\Gamma(CH_2)$	533	A″	$\nu(CF)_a$	1138	$\Gamma(CCH)+\nu(CC)$	632	$\rho(CH_2)_s+\Gamma(CCH)$	634
ν_{13}	A″	$\tau(CH_3)$	988	$\delta(CCF)$	465	A″	$\tau(CH_2)$	918	$\delta(CCF)_s$	469	$\delta(CCF)_s$	472
ν_{14}	A″	$\delta(CCF)$	376	$\Gamma(CH_2)$	361	A″	$\delta(CCF)$	395	$\delta(CCF)_a$	311	$\delta(CCF)_a$	285
ν_{15}	A″	torsion	200	torsion	132	A″	torsion	93	torsion	128	torsion	84

^{a} ν-stretch; δ-bend; ρ-rock; ω-wagging; τ-twist; Γ-pyramidal distortion. ^{b} Calculated at MP2/6-311+G(2d,p) level. ^{c} ν-stretch; δ-bend; ρ-rock; ω-wagging; τ-twist; Γ-pyramidal distortion. ^{d} Calculated at MP2/6-311+G(2d,p) level.
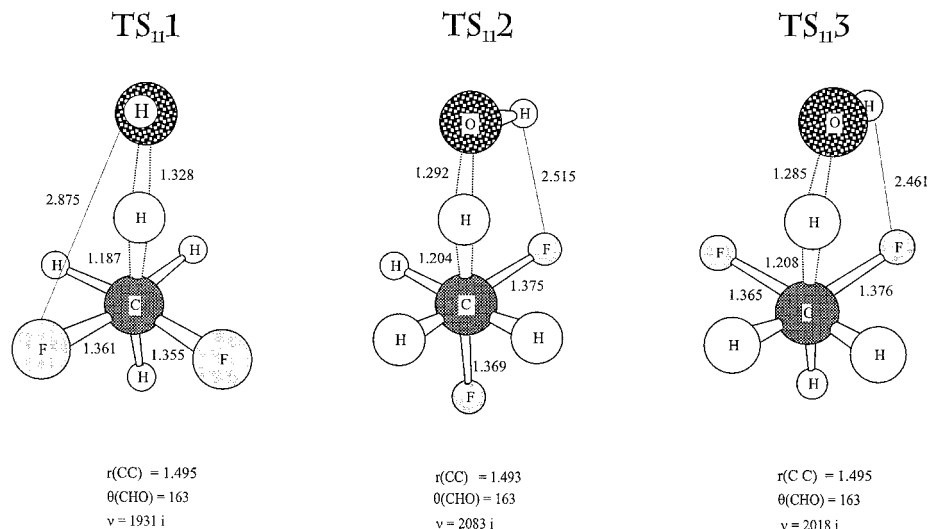
Tropospheric Reactivity of Fluorinated Ethanes

J. Phys. Chem. A, Vol. 105, No. 10, 2001 **1973**

Figure 1. Selected geometrical parameters (bond lengths in Å and angles in degrees) and imaginary vibration frequencies (cm^{-1}) for the transition-state structures of 1,1-difluoroethane reaction with OH radical.
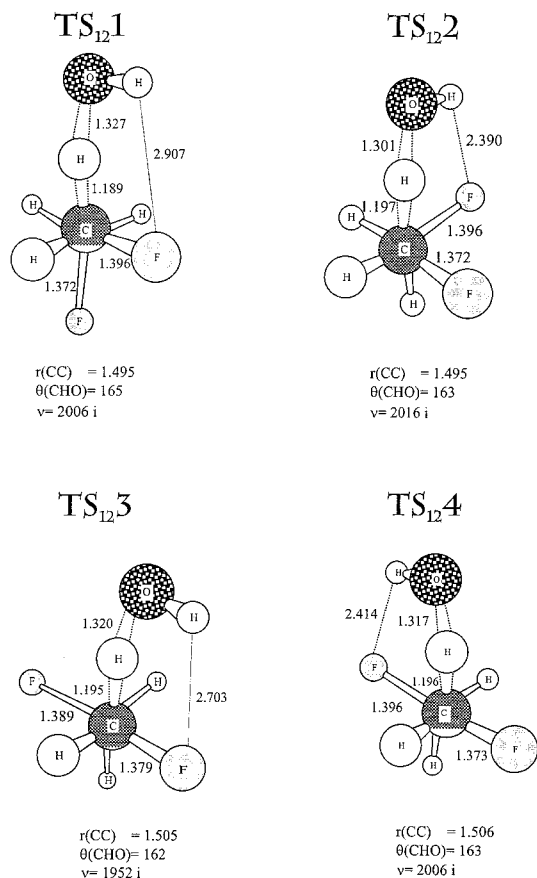
Figure 2. Selected geometrical parameters (bond lengths in Å and angles in degrees) and imaginary vibration frequencies (cm^{-1}) for the transition-state structures of 1,2-difluoroethane reaction with OH radical.

C—F distances are shorter and "1,2" distances are longer than are equilibrium distances in the 1,2-difluoroethane due to the electron density redistribution where the polarity of the former bond is increased and the polarity of the latter is decreased.

The normal mode of the imaginary frequency corresponds to the transfer of hydrogen atom between carbon and oxygen atoms. The lowest modes correspond to the van der Waals frequencies of the OH relative to the fluorocarbon moiety, followed by the OH hindered rotation. The rest of the modes are vibrations of the fluorocarbon moiety coupled with the

motions of the reactive H···O···H group. A complete listing of the calculated vibration frequencies for all transition-state structures is given in Supporting Information (Table S1). The imaginary frequencies are given in Figures 1 and 2.

C. Reactive Complexes. A number of van der Waals complexes were found, as shown in Schemes 1 and 2. For R1 reaction three Cx^R and two Cx^P complexes were found. The most important geometrical parameters are given in Figure 3. The geometries of reactants and products are only slightly perturbed in the complexes. The largest change is elongation of the C—F bond caused by the formation of the hydrogen bond. The H···F distances are much shorter than in the TS structures; 2.086, 2.094, and 2.136 Å for the Cx$_{11}^R$1, Cx$_{11}^R$2, and Cx$_{11}^R$3, and 2.213 and 2.217 Å for the Cx$_{11}^P$1 and Cx$_{11}^P$2, respectively.

Three Cx^R and four Cx^P complexes were found for the R2 reaction. The Cx$_{11}^R$1 and Cx$_{11}^R$2 are formed from the gauche conformer and the Cx$_{11}^R$3 from the anti conformer interaction with OH radical. As in the case of the R1 complexes, reactant and product geometries are only slightly perturbed with the asymmetry of the C—F bonds caused by formation of the H-bond. Distances between fluorine atom and the hydrogen atom from the OH radical are even shorter than in the case of the "1,1" complexes: 1.985, 2.102, and 2.027 Å for the Cx$_{12}^R$1, Cx$_{12}^R$2, and Cx$_{12}^R$3, and 2.218, 2.079, 2.278, and 2.099 Å for the Cx$_{12}^P$1, Cx$_{12}^P$2, Cx$_{12}^P$3, and Cx$_{12}^P$4. In the product-like complexes, additional stabilization is achieved through the interaction of the oxygen atom from the water molecule and one of the hydrogens from the radical moiety, i.e., another weak hydrogen bond is formed. Distances between these atoms are still smaller than the sum of the van der Waals radii[39] (see Figures 3 and 4).

Vibrational frequencies of all van der Waals complexes are listed in supporting information (Table S2). The first few vibrational frequencies correspond to the van der Waals modes, and because the anharmonicity is not taken into account, those modes are subject to the largest error. Other modes keep the analogy with those of separated species.

2. Features of the Ab Initio Potential Energy Function. Complete energetics for reactions R1 and R2 are given in Table 4, and the definition of the relative energies is given in Scheme 3. All three reactant-like complexes formed in the reaction R1 are of the similar stability, the difference in energies being only 0.3 kcal mol^{-1} between Cx$_{11}^R$1 and Cx$_{11}^R$3. Complex Cx$_{11}^R$3 is
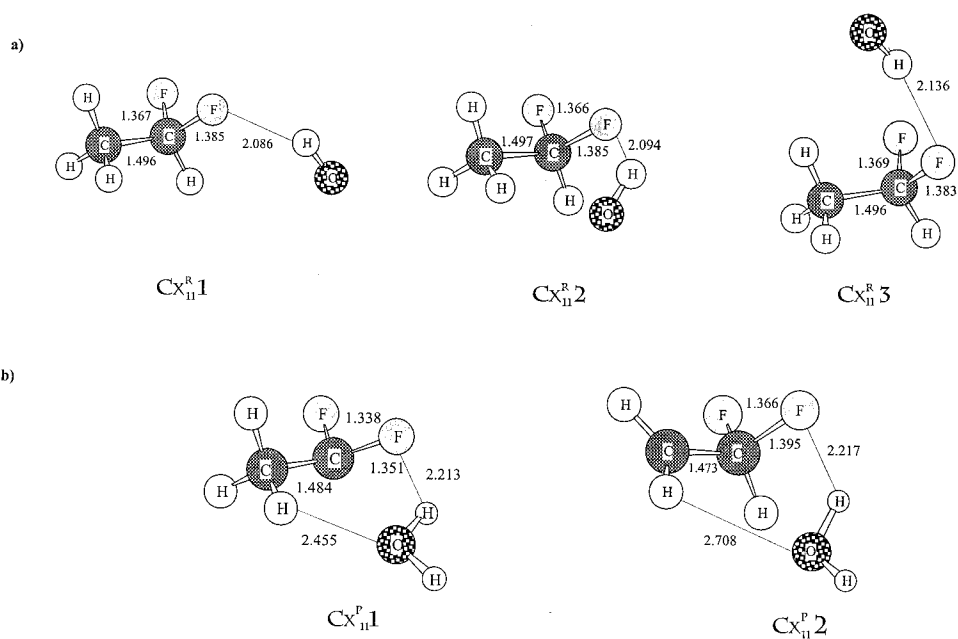
Figure 3. Selected geometrical parameters (Å) for (a) reactant and (b) product complexes of 1,1-difluoroethane reaction with OH radical.
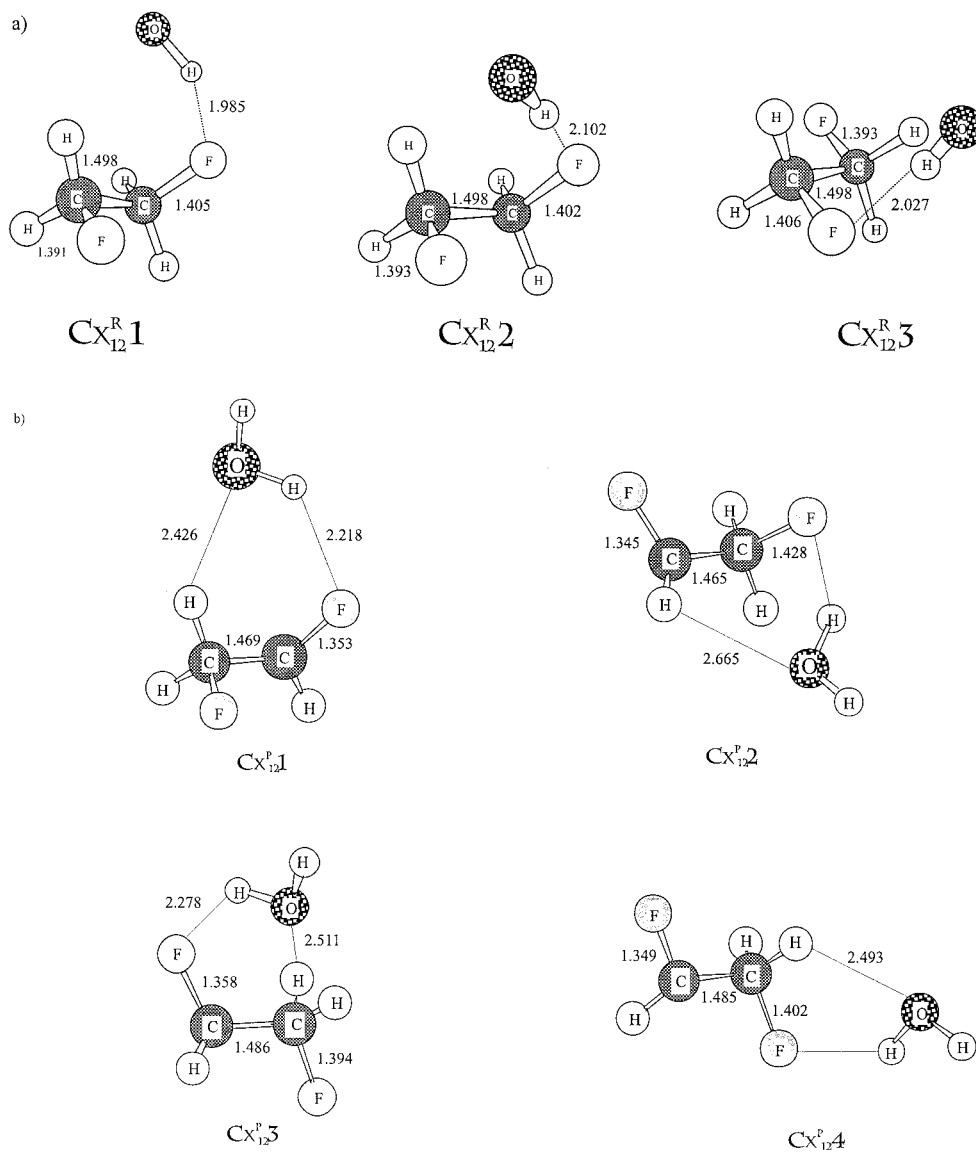
Figure 4. Selected geometrical parameters (Å) for (a) reactant and (b) product complexes of 1,2-difluoroethane reaction with OH radical.

Tropospheric Reactivity of Fluorinated Ethanes

J. Phys. Chem. A, Vol. 105, No. 10, 2001 **1975**

**TABLE 4: Energetics for 1,1- and 1,2-Difluoroethane Reactions with OH Radical Calculated at MP2/bs2 Level (kcal mol^{-1})^g**

1,1-Difluoroethane			
energies	reactive species^{a,b}		
ΔE_{cx}^{R}	**Cx$_{11}^{R}$1** −2.3 (−2.4)	**Cx$_{11}^{R}$2** −2.4 (−2.4)	**Cx$_{11}^{R}$3** −2.6 (−2.7)
$\Delta E^{\ddagger c}$	**TS$_{11}$1** 2.3 (4.0)	**TS$_{11}$2** 3.7 (5.1)	**TS$_{11}^{1}$3** 3.8 (5.2)
ΔE_{cx}^{P}	**Cx$_{11}^{P}$1** 2.4 (2.6)	**Cx$_{11}^{P}$2** 3.2 (3.6)	
$\Delta_r H^d$	**P$_{11}$1** −21.3 (−18.7)	**P$_{11}$2** −17.9 (−15.4)	

1,2-Difluoroethane				
energies	reactive species^{e,f}			
ΔE_{R}^{cx}	**Cx$_{12}^{R}$1** −3.0 (−2.9)	**Cx$_{12}^{R}$2** −3.0 (−3.1)	**Cx$_{12}^{R}$3** −2.6 (−2.5)	
$\Delta E^{\neq}$	**TS$_{12}$1** 2.5 (3.9)	**TS$_{12}$2** 2.2 (3.7)	**TS$_{12}$3** 3.2 (4.7)	**TS$_{12}$4** 2.8 (4.3)
ΔE_{P}	**Cx$_{12}^{P}$1** 2.3 (2.7)	**Cx$_{12}^{P}$2** 3.8 (4.1)	**Cx$_{12}^{P}$3** 2.5 (2.8)	**Cx$_{12}^{P}$4** 2.6 (2.7)
$\Delta_r H$	P$_{12}$1 −22.8 (−20.3)	P$_{12}$2 −21.5 (−18.9)		

^{a} Calculated according to Scheme 1. ^{b} $\Delta E(P_{11}1\text{-}P_{11}2) = 3.40\ (−3.24)$. ^{c} $E_a = 2.1\pm0.3$, and 1.9 ± 0.5 kcal mol^{-1}(ref 1). ^{d} $\Delta_r H^{exp}(P_{11}1) = −20.7$ kcal mol^{-1} (ref 20). ^{e} Calculated according to Scheme 2. ^{f} $\Delta E(R_{12}1 − R_{12}2) = −0.9\ (−0.9)$ $\Delta E(P_{12}1 − P_{12}2) = −2.2\ (−2.3)$. ^{g} Values in parentheses are calculated at the MP2/bs1 level.

SCHEME 3. Description of the Relative Energies Given in Tables 3 and 4
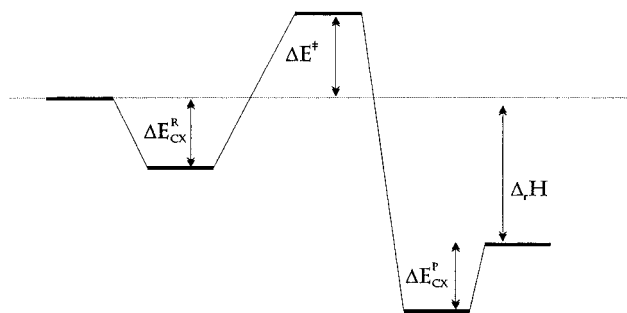
2.6 kcal mol^{-1} more stable than the separated reactant molecules. Reactant-like complexes formed in the R2 reaction are slightly more stable than those from reaction R1. On the other hand, stabilization of the product-like complexes is somewhat larger in both reactions. Complex Cx$_{11}^{P}$2 is the most stable of the "1,1" complexes, with stabilization energy of 3.2 kcal mol^{-1} with respect to the products. Complex Cx$_{12}^{P}$2 is the most stable of the "1,2" complexes with stabilization energy of 3.8 kcal mol^{-1}.

From the three possible reaction channels in the R1 reaction, the one that goes through the TS$_{11}$1 is the most reactive with the barrier of 2.3 kcal mol^{-1}. The other two transition-state structures lie 3.7 and 3.8 kcal mol^{-1} higher than the reactant molecules. This is in agreement with the larger stability of the P$_{11}$1 radical indicating the weaker α C−H bond. Therefore, TS$_{11}$1 is the bottleneck of the reaction R1. The calculated reaction barrier of 2.3 kcal mol^{-1} is in excellent agreement with the activation energy of 2.1±0.3, and 1.9±0.5 kcal mol^{-1} calculated from the temperature dependence of the rate constants.[1]

For the R2 reaction, barrier heights are 2.5, 2.2, 3.2, and 2.8 kcal mol^{-1}. The larger number of the possible pathways with similar barriers for the reaction R2 indicate the larger reaction rates than for the reaction R1, in agreement with experimental findings.

It is interesting to note that relative energies calculated with bs1 are close to those calculated with bs2 for the van der Waals complexes, whereas for the transition-state structures and product radicals, additional stabilization of ~1.5 and 2.5 kcal mol^{-1} is gained (Table 4).

Projection of spin contamination lowered the reaction barriers by approximately 3 kcal mol^{-1}. Reaction enthalpies are less sensitive to the spin projection (~1 kcal mol^{-1}) because the spin contamination of the product radical is smaller.

3. Features of the PM3-SRP Potential Energy Function. The reactive C−H and O−H distances, imaginary frequencies, energy barriers and reaction enthalpies calculated at both ab initio, PM3 and PM3-SRP levels, are compared in Table 5. Barriers calculated at the PM3 level are overestimated about 2.5 times in comparison with the MP2/bs2 results. PM3-SRP results are between the values obtained with bs1 and bs2, respectively. Similar results are obtained for the reaction enthalpies, only the values for the reaction R2 are somewhat too large. PM3-SRP reactive distances are about 3% longer and imaginary frequencies are from 10 to 20% higher than the ab initio ones for all transition-state structures.

It is important to stress that the PM3-SRP method failed to describe properly the hydrogen abstraction from the α-carbon of the 1,1-difluoroethane. Too large stabilization of the transition-state structure and the corresponding product radical result in barriers that are too low and reaction enthalpies that are too large. However, as we found out this is not only the deficiency of the SRP model but of a minimal basis set approximation. The same results are obtained with the PM3 Hamiltonian as well as at the UHF and MP2 levels when the minimal STO-3G basis set was used. Within the minimal basis set framework, the electronegativity of the fluorine atom is too small, so the electron density is donated to the C atom resulting in the artificial stabilization. For example, the delocalization energy between natural bond orbitals of the fluorine lone pair and empty antibonding orbital of C radical atom is 26 kcal mol^{-1} at the UHF/6-311+G(2d,p) level and 38 kcal mol^{-1} at the UHF/STO-3G level. The same pattern is obtained for the MP2 wavefunction.

Actually, the same behavior was obtained in our last paper for the fluoroethane reaction with OH radical[4d] where too low barriers and consequently too large reaction rate constants were obtained at the PM3-SRP level. To correct for discrepancies between SRP and ab initio values, we introduced the correction factors. At that time the correct reason for the overestimation of the rate constants was not clear, and it was concluded that the source of error is in the use of the SRP parameters fitted to the ethane reaction with the OH radical.

4. Rate Constants. Reaction rate constants calculated at 298 K for all reaction pathways of reactions R1 and R2 together with experimental values are given in Table 6. The MP2///SRP rate constants are in very good agreement with the experimental rate constants, whereas the SRP results indicate a trend similar to that for the fluoroethane and chloroethane reactions with OH radical. For reaction R2, SRP results are 1 order of magnitude larger than the experimental values. The results corrected by the scaling factor calculated for the fluoroethane reaction[4d] are close to the MP2/SRP results. Thus, the correction factor determined for the monofluorinated ethane is suitable for the

TABLE 5: Barrier Heights (kcal mol⁻¹), Reaction Enthalpies (kcal mol⁻¹), Reactive Bond Lengths (Å), and Imaginary Vibration Frequencies (cm⁻¹) Calculated at the ab Initio and Semiempirical Levels of Theory for the 1,1-Difluoroethane and 1,2-Difluoroethane Reaction with OH Radical

1,1-Difluoroethane						1,2-Difluoroethane					
method	ΔE^a	$\Delta_r H$	r_{CH}	r_{OH}	v_i	method	ΔE^a	$\Delta_r H$	r_{CH}	r_{OH}	v_i
			$TS_{11}1$						$TS_{12}1$		
MP2/bs1	4.0	−18.7	1.187	1.328	1931	MP2/bs1	3.9	−20.3	1.189	1.327	1884
MP2/bs2	2.5	−21.3				MP2/bs2	2.5	−22.8			
PM3-SRP	1.9	−31.7	1.238	1.390	2428	PM3-SRP	3.6	−26.9	1.224	1.356	2382
PM3	6.0	−33.1	1.254	1.370	2610	PM3	7.5	−29.5	1.235	1.342	2554
			$TS_{11}2$						$TS_{12}2$		
MP2/bs1	5.1	−15.4	1.204	1.292	2083	MP2/bs1	3.7	−20.3	1.197	1.301	2016
MP2/bs2	3.7	−17.9				MP2/bs2	2.2	−22.8			
PM3-SRP	6.6	−16.1	1.215	1.309	2270	PM3-SRP	3.3	−26.9	1.224	1.360	2377
PM3	10.3	−20.1	1.223	1.304	2426	PM3	7.2	−29.5	1.235	1.346	2554
			$TS_{11}3$						$TS_{12}3$		
MP2/bs1	5.2	−15.4	1.208	1.285	2018	MP2/bs1	4.7	−18.9	1.195	1.320	1952
MP2/bs2	3.8	−17.9				MP2/bs2	3.2	−21.5			
PM3-SRP	6.3	−16.1	1.215	1.312	2266	PM3-SRP	3.5	−26.9	1.225	1.362	2376
PM3	10.0	−20.1	1.224	1.308	2440	PM3	7.5	−29.7	1.238	1.345	2563
									$TS_{12}4$		
						MP2/bs1	4.3	−18.9	1.196	1.317	2006
						MP2/bs2	2.8	−21.5			
						PM3-SRP	3.5	−26.9	1.227	1.362	2384
						PM3	7.8	−29.7	1.242	1.348	2640

TABLE 6: Reaction Rate Constants for 1,2-Difluoroethane and 1,1-Difluoroethane Reaction with OH Radical Calculated at 298 K

1,2-Difluoroethane				
	SRP		MP2///SRP	
$k*10^{13}$	$k^{298}_{CVT/\mu OMT}$	$k^{298}_{CVT/LCT}$	$k^{298}_{CVT/\mu OMT}$	$k^{298}_{CVT/LCT}$
TS1	1.66	0.83	0.88	0.60
TS2	2.29	1.11	0.51	0.34
TS3	4.38	2.16	0.79	0.54
TS4	4.76	2.32	0.62	0.42
sum	13.09	6.42	2.81	1.90
corr.[a]	2.92	1.46		
corr.[b]	2.81	1.90		
exp.	1.12[c]			

1,1-Difluoroethane				
	SRP		MP2///SRP	
$k*10^{14}$	$k^{298}_{CVT/\mu OMT}$	$k^{298}_{CVT/LCT}$	$k^{298}_{CVT/\mu OMT}$	$k^{298}_{CVT/LCT}$
TS1	132.08	85.79	8.07	4.94
TS2	0.40	0.28	0.57	0.38
TS3	0.72	0.54	1.08	0.81
Corr2[d]	8.31	5.17		
exp.	3.76[e]			

[a] Correction factor of 0.223 and 0.228 for CVT/μOMT and CVT/LCT SRP results calculated as a ratio between MP2///SRP and SRP results for fluoroethane reaction with OH radical (ref 4d). [b] Correction factor of 0.215 and 0.292 for CVT/μOMT and CVT/LCT SRP results calculated as a ratio between MP2///SRP and SRP results for reaction R2. [c] Reference 1. [d] Correction factor of 0.061 and 0.058 for CVT/μOMT and CVT/LCT SRP results calculated as a ratio between MP2///SRP and SRP results for reaction R1 used for the TS1 pathway, and correction factor of 0.215 and 0.292 for CVT/μOMT and CVT/LCT SRP results calculated as a ratio between MP2///SRP and SRP results for reaction R2 used for the TS2 and TS3 pathways. [e] Reference 1.

1,2-difluoroethane as well. For the reaction R1, the situation is somewhat different. Due to the failure of the minimal basis set method to describe the stability of the "1,1" radicals and transition-state structures, the reaction barriers for the reaction pathway passing through $TS_{11}1$ are significantly underestimated and the rate constant is consequently overestimated for more than 1 order of magnitude. Applying correction factor for fluorethane results in rate constants that are still about 5–8 times too large.

From these results it is clear that fluoroethane was a good model for 1,2-difluoroethane but not for 1,1-difluoroethane. Because we would like these scaling factors to be consistent and general, the new scaling factors are calculated as a ratio from the MP2///SRP and SRP rate constants for both R1 and R2 reactions. The new scaling factors are given in Table 6.

An analogous procedure, using the same scaling factors as for the difluoroethane, is applied to the test suite of all polyfluorinated ethanes. Results are shown in Table 7. The reported rates are sums of the individual rates for each reaction pathway scaled with the corresponding scaling factor. If there is one fluorine atom at the site of hydrogen abstraction the scaling factor for the 1,2-difluoroethane reaction was used, and if there were two fluorine atoms the scaling factor for the 1,1-difluoroethane reaction was used. Following the described procedure, room-temperature rate coefficients were predicted within a factor of 3 for all hydrofluoroethanes.

The temperature dependence (200−800 K) of the reaction rate constants for the reaction R1 and reaction R2 calculated at the different levels are given in Figure 5. The experimental rate coefficients for 1,1-difluoroethane are available only for a temperature region from 200 to 400 K. For 1,2-difluoroethane, the temperature dependence of the rate coefficient is not measured yet. Therefore, our calculations provide the first prediction of temperature profiles of the rate coefficients for both 1,1- and 1,2-difluoroethane.

LCT and μOMT tunneling approximations overestimate the tunneling at the low temperatures, resulting in larger disagreement with the experimental data for the temperature range from 200 to 250 K. However, good agreement is obtained between experimental and calculated data when simple Wigner tunneling correction is used, because linear temperature dependence of the experimental rate coefficients is observed for this temperature range. Analogous behavior was observed for the fluoroethane and chloroethane reaction with OH radical,[4d] only there, while the reaction rates were underestimated, the resulting effect was a better agreement with the experiment at the lower temperatures. For the higher temperatures (250−800 K), all three tunneling methods predict experimental rate coefficients within a factor of 2. SRP-corr results follow the ab initio ones in the whole temperature range, showing that proposed correction

Tropospheric Reactivity of Fluorinated Ethanes

J. Phys. Chem. A, Vol. 105, No. 10, 2001 **1977**

TABLE 7: SRP Reaction Rate Constants for the OH Radical Reaction with a Complete Set of Tri-, Tetra-, and Penta-substituted Fluoroethanes

$k*10^{14}$	CH$_3$CF$_3$		CH$_2$FCHF$_2$		CH$_2$FCF$_3$		CHF$_2$CHF$_2$		CHF$_2$CF$_3$	
	$k^{298}_{CVT/\mu OMT}$	$k^{298}_{CVT/LCT}$	$k^{298}_{CVT/\mu OMT}$	$k^{298}_{CVT/LCT}$	$k^{298}_{CVT/\mu OMT}$	$k^{298}_{CVT/LCT}$	$k^{298}_{CVT/\mu OMT}$	$k^{298}_{CVT/LCT}$	$k^{298}_{CVT/\mu OMT}$	$k^{298}_{CVT/LCT}$
TS1	0.50	0.34	0.97	0.66	4.31	2.51	0.59	0.36	0.35	0.24
TS2	0.11	0.08	1.94	1.32	0.96	0.56	0.79	0.46	0.08	0.06
TS3			1.81	1.02						
TS4			2.21	1.54						
TS5			2.32	1.38						
corr.[a]	0.13	0.13	9.25	5.92	1.33	0.90	1.38	0.82	0.43	0.29
exp.[b]	0.13		1.83		0.49 and 0.85		0.59		0.19	

[a] Correction factor of 0.061 and 0.058, and 0.215 and 0.296 for CVT/μOMT and CVT/LCT SRP results of reactions R1 and R2 (see Table 6). [b] Reference 1.

(a)

(b)
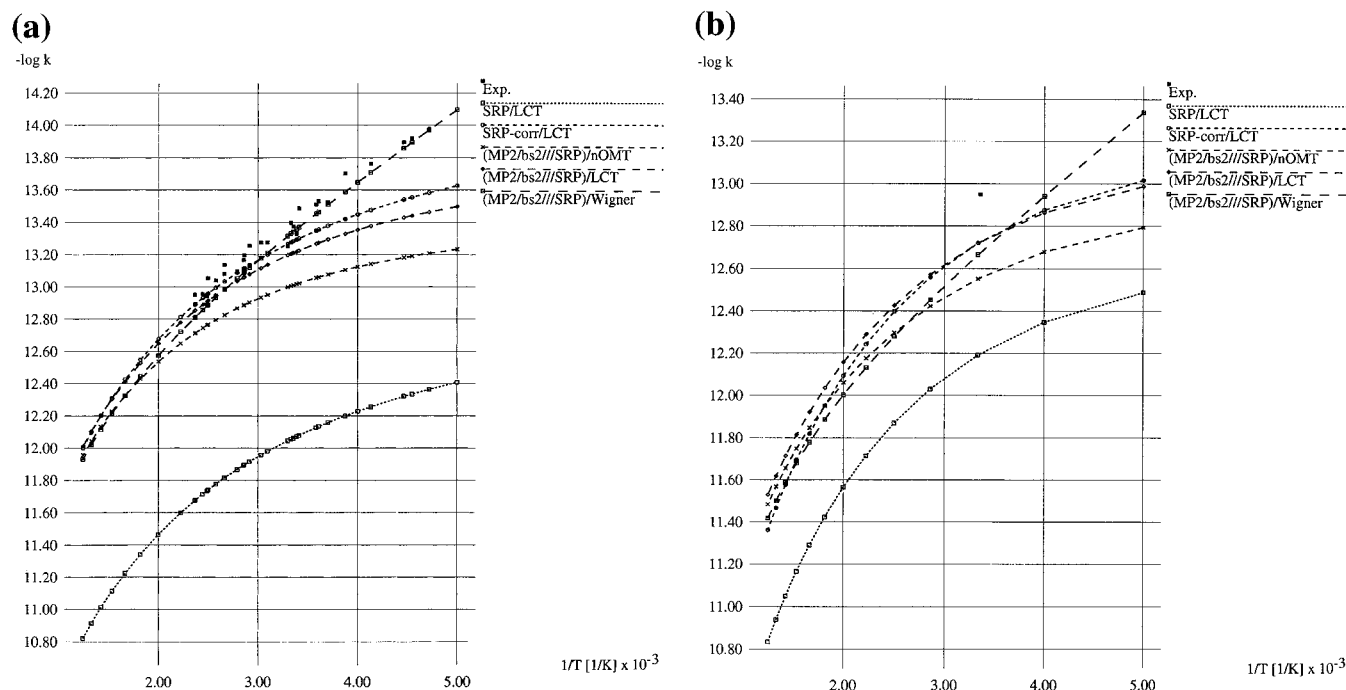
Figure 5. Temperature dependence of the experimental and calculated reaction rate constants for the (a) 1,1-difluoroethane, and (b) 1,2-difluoroethane reaction with OH radical.

factors are only slightly temperature dependent and can be used for estimation of the rate coefficients for the larger hydrocarbons within the broad temperature range.

From the theoretical point of view, one would expect to obtain more accurate tunneling contributions going from Wigner, SCT, LCT to μOMT methods. However, it is still not clear whether our results reflect shortcomings of the dynamics or of the SRP potential. Further investigations are needed to explain this result.

Conclusions

In this paper, the detailed study of hydrogen atom abstraction from 1,1- and 1,2- difluoroethane is reported. Results are based on high-level electronic structure calculations and dual-level direct dynamic calculations with multidimensional semiclassical tunneling corrections. Altogether, 26 stationary points were found, corresponding to the three reaction channels for 1,1- and four reaction channels for 1,2-difluoroethane, respectively. Both reactions follow an indirect mechanism forming the pre-reaction complexes on the both sides of the reaction path.

From the three reaction channels of the R1 reaction, the one with the barrier height of 2.3 kcal mol^{-1} is the rate determining step. The other two channels have 1.5 kcal mol^{-1} higher reaction barriers. For the reaction R2, two reaction channels have competitive barrier heights whereas the other two are 0.6 and 1 kcal mol^{-1} higher than the bottleneck barrier.

Direct dynamics study was based on the semiempirical PM3 Hamiltonian using specific reaction parameters (SRP) derived for the ethane reaction with OH radical. Reaction energetics were corrected with the ab initio data calculated for all stationary points at the MP2/6-311++G(3df,2pd) level, whereas the geometries and frequencies were calculated at MP2/6-311+G-(2d,p) level.

Satisfactory agreement between SRP and ab initio data was obtained for 1,2-difluorethane. The corresponding rate SRP constants were additionally scaled in order to match the ab initio ones, as was already suggested in the case of fluoroethane. For 1,1-difluoroethane the reaction barriers for the TS$_{11}$1 are highly underestimated due to the failure of the minimal basis set approximation to describe the stability of the "1,1" radicals and transition-state structures. Consequently, reaction coefficients were overestimated by more than 1 order of magnitude. Therefore, two scaling factors were calculated as a ratio between the MP2///SRP and SRP rate constants for each reaction.

Although this procedure is empirical, with respect to reoptimized PM3 Hamiltonian and introduced scaling factors, it is very helpful for estimating reaction rate coefficients for the fluorinated hydrocarbons within a factor of 3 in a broad temperature range.

Our results show that SRP can be used as a general reaction parameters for analogous reactions. Further improvement can

1978 *J. Phys. Chem. A, Vol. 105, No. 10, 2001*

Sekušak and Sabljić

be achieved by introducing the scaling factors calculated as a ratio between SRP and MP2/SRP rate constants for the simplest reaction (in this case difluoroethane). The scaling factors can further be used for the more complicated compounds within the class. The procedure is tested on the test suite of all polyfluorinated hydrocarbons and can further be applied to predict reaction rate coefficients of larger fluorinated hydrocarbons.

Multidimensional tunneling approximations such as LCT and μOMT tend to overestimate tunneling corrections for the low temperatures. For the 1,1-difluorethane reaction with OH radical, experimental temperature dependence of the rate coefficients is best reproduced when the simple Wigner formula was used for the tunneling correction.

Supporting Information Available: Supporting Information Available. Complete listing of the calculated vibration frequencies for all transition-state structures (Table S1) and vibrational frequencies of all van der Waals complexes (Table S2). This material is available free of charge via the Internet at http://pubs.acs.org.

References and Notes

(1) (a) Atkinson, R. *Chem. Rev.* **1986**, *86*, 69. (b) Atkinson, R. *J. Phys. Chem. Ref. Data Monograph 1*, 1989. (c) Atkinson, R.; Baulch, D. L.; Cox, R. A.; Hampson Jr., R. F.; Kerr, J. A.; Troe, J. *J. Phys. Chem.* **1989**, *18*, 881. (d) Atkinson, R. *J. Phys. Chem. Ref. Data Monograph 2*, 1994.

(2) Barker, J. R. Ed. *Progress and problems in atmospheric chemistry*, Advanced Series in Physical Chemistry 3; World Scientific Publishing Co.: Singapore, 1995.

(3) (a) Hayman G. D.; Derwent R. G. *Environ. Sci. Technol.* **1997**, *31*, 327. (b) Rowland, F. S. *Angew. Chem., Intl. Ed.* **1996**, 35, 1786.

(4) (a) Sekušak *J. Chem. Phys.* **1995**, *102*, 7504. (b) Sekušak *J. Phys. Chem.* **1996**, *100*, 6212; Erratum, **1997**, *101*, 967. (c) Sekušak *J. Phys. Chem. A* **1997**, *101*, 4245. (d) Sekušak *J. Phys. Chem. A* **1999**, *103*, 11394.

(5) (a) Dorigo, A. E.; Houk, K. N. *J. Org. Chem.* **1988**, *53*, 1650. (b) Truong, T. N.; Truhlar, D. G. *J. Chem. Phys.* **1990**, *93*, 1761. (c) Gonzales, C.; McDouall, J. J. W.; Schlegel, H. B. *J. Phys. Chem.* **1990**, *94*, 7467. (d) Lasaga, A. C.; Gibbs, G. V. *Geophys. Res. Lett.* **1991**, 18, 1217. (e) Dobbs, K. D.; Dixon, D. A.; Komornicki, A. *J. Chem. Phys.* **1993**, *98*, 8852.

(6) Bottoni, A.; Poggi, G.; Emmi, S. S. *J. Mol. Struct. (THEOCHEM)* **1993**, *279*, 299. (b) Espinosa-Garcia, J.; Coitino, E. L.; Gonzalez-Lafont, A.; Lluch, J. M. *J. Phys. Chem.* **1998**, *102*, 10715. (c) Maity, D. K.; Duncan, W. T.; Truong, T. N. *J. Phys. Chem A* **1999**, *103*, 2152. (d) Louis, F.; Gonzalez, C. A.; Huie, R. E.; Kurylo, M. J. *J. Phys. Chem. A* **2000**, *104*, 2931.

(7) (a) Melissas, V. S.; Truhlar, D. G. *J. Phys. Chem.* **1994**, *98*, 875. (b) Martell, J. M.; Mehta, A. K.; Pacey, P. D.; Boyd, R. J. *J. Phys. Chem.* **1995**, *99*, 8661.

(8) (a) Martell, J. M.; Boyd, R. J. *J. Phys. Chem.* **1995**, *99*, 13402. (b) Chandra, A. K.; Uchimaru, T. *J. Phys. Chem. A* **1999**, *103*, 10874.

(9) Hu, W.-P.; Rossi, I.; Corchado, J. C.; Truhlar, D. G. *J. Phys. Chem. A* **1997**, *101*, 6911.

(10) Truhlar D. G.; Isaacson A. D.; Garrett B. C. *Theory of Chemical Reaction Dynamics*; M. Baer, Ed.; CRC Press: Boca Raton, 1985, *4*, 65.

(11) Truhlar, D. G., Heidrich D., Eds. *The Reaction Path in Chemistry: Current Approaches and Perspectives*; Kluwer: Dordrecht, 1995; p 229.

(12) Truhlar, D. G.; Garrett, B. C.; Klippenstein, S. J. *J. Phys. Chem.* **1996**, *100*, 12771.

(13) Truhlar, D. G.; Isaacson, A. D.; Skodje, R. T.; Garrett, B. C. *J. Phys. Chem.* **1982**, *86*, 2252.

(14) Garrett, B. C.; Joseph, T.; Truong, T. N.; Truhlar, D. G. *J. Chem. Phys.* **1989**, *136*, 271.

(15) Moller, C.; Plesset, M. S. *Phys. Rev.* **1934**, *46*, 618.

(16) Sekušak, S.; Sabljić, A., unpublished results.

(17) (a) Krishnan R.; Binkley J. S.; Seeger R.; Pople J. A. *J. Chem. Phys* **1980**, *72*, 650. (b) Clark T.; Chandrasekhar J.; Spitznagel G. W.; Schleyer P. v. R. *J. Comput. Chem.* **1983**, *4*, 294.

(18) Frisch, M. J.; Pople, J. A.; Binkley, J. S. *J. Chem. Phys.* **1984**, *80*, 3265.

(19) Schlegel, H. B. *J. Phys. Chem.* **1988**, *92*, 3075.

(20) Frisch, M. J.; Trucks, G. W.; Schlegel, H. B.; Gill, P. M. W.; Johnson, B. G.; Robb, M. A.; Cheesman, J. R.; Keith, T.; Petersson, G. A.; Montgomery, J. A.; Raghavachari, K.; Al-Laham, M. A.; Zakrzewski, V. G.; Ortiz, J. V.; Foresman, J. B.; Cioslowski, J.; Stefanov, B. B.; Nanayakkara, A.; Challacombe, M.; Peng, C. Y.; Ayala, P. Y.; Chen, W.; Wong, M. W.; Andres, J. L.; Replogle, E. S.; Gomperts, R.; Martin, R. L.; Fox, D. J.; Binkley, J. S.; Defrees, D. J.; Baker, J.; Stewart, J. J. P.; Head-Gordon, M.; Gonzalez, C.; Pople, J. A. *Gaussian 94, Revision C.2.* Gaussian, Inc.: Pittsburgh, PA, 1995.

(21) (a) Glendening, E. D.; Reed, A. E.; Carpenter, J. E.; Weinhold, F. NBO Program, Version 3.1. (b) Reed, A. E.; Curtiss, L. A.; Weinhold, F. *Chem. Rev.* **1988**, *88*, 3250.

(22) (a) Hu, W.-P.; Liu, Y.-P.; Truhlar, D. G. *J. Chem. Soc., Faraday. Trans.* **1994**, *90*, 1715. (b) Corchado, J. C.; Espinosa-Garcia, J.; Hu, W.-P.; Rossi, I.; Truhlar, D. G. *J. Phys. Chem.* **1995**, 99, 4618.

(23) Parrinello, M. *MOTEC: Modern Techniques in Computational Chemistry*; Clementi, E., Ed.; ESCOM: Leiden, 1991; p 833.

(24) Gonzalez-Lafont, A.; Truong, T. N.; Truhlar, D. G. *J. Phys. Chem.* **1991**, *95*, 4618.

(25) Schmidt, M. W.; Gordon, M. S.; Dupuis, M. *J. Am. Chem. Soc.* **1985**, *107*, 2585.

(26) (a) Garrett, B. C.; Redmon, M. J.; Steckler, R.; Truhlar, D. G.; Baldridge, K. K.; Bartol, D.; Schmidt, M. W.; Gordon, M. S. *J. Phys. Chem.* **1988**, 92, 1476. (b) Melissas, V. S.; Truhlar, D. G.; Garrett, B. C. *J. Chem. Phys.* **1992**, *96*, 5758.

(27) (a) Hu, W.-P.; Liu, Y.-P.; Truhlar, D. G. *J. Chem. Soc., Faraday. Trans.* **1994**, *90*, 1715. (b) Corchado, J. C.; Espinosa-Garcia, J.; Hu, W.-P.; Rossi, I.; Truhlar, D. G. *J. Phys. Chem.* **1995**, *99*, 4618.

(28) (a) Steckler, R.; Hu, W.-P.; Liu, Y.-P.; Lynch, G. C.; Garrett, B. C.; Isaacson, A. Lu, D.-H.; Melissas, V. S.; Truong, T. N.; Rai, S. N.; Hancock, G. C.; Lauderdale, J. G.; Joseph, T.; Truhlar, D. G. *POLYRATE version 7.8.1*, University of Minnesota, Minneapolis, 1998. (b) Lu, D.-H.; Truong, T. N.; Melissas, V. S.; Lynch, G. C.; Liu, Y.-P.; Garrett, B. C.; Steckler, R.; Isaacson, A. D.; Rai, S. N.; Hancock, G. C.; Lauderdale, T J. G.; Joseph, T.; Truhlar, D. G. *Comput. Phys. Commun.* **1992**, *71*, 235.

(29) Liu, Y.-P.; Lu, D.-H.; Gonzalez-Lafont, A.; Truhlar, D. G.; Garrett, B. C. *J. Am. Chem. Soc.* **1993**, *115*, 7806.

(30) *CRC Handbook of Chemistry and Physics*, 79th ed., Lide, D. R., Ed., CRC Press: Boca Raton, FL, 1998−1999.

(31) Chuang, Y.-Y.; Fast, P. L.; Hu, W.-P.; Lynch, G. C.; Liu, Y.-P.; Truhlar, D. G. *MORATE Version7.5*, University of Minnesota, Minneapolis, 1997.

(32) Sekušak, S.; Sabljić, A. *Chem. Phys. Lett.* **1997**, *272*, 353.

(33) Durig, J. R.; Liu, J.; Little, T. S.; Kalasinsky, V. F. *J. Phys. Chem.* **1992**, *96*, 8224.

(34) Engkvist, O.; Karlstroem, G.; Widmark, P.-O. *Chem. Phys. Lett.* **1977**, *265*, 19.

(35) (a) Chase, M. W., Jr.; Davies, C. A.; Downey, J. R., Jr.; Fruip, D. J.; McDonald, R. A.; Syverud, A. N. Eds.; *JANAF* Thermochemical Tables, 3rd ed.; National Bureau of Standards: Washington, D.C., 1985; Vol. 14. (b) Takeo, H; Matsumura, C.; Morino, Y. *J. Chem. Phys.* **1986**, *84*, 4205. (c) Freisen, D.; Hedberg, K. *J. Am. Chem. Soc.* **1980**, *102*, 3987. (d) Craig, N. C.; Chen, A.; Suh, K. H.; Klee, S.; Mellau, G. C.; Winnewisser B. P.; Winnewisser, M.; *J. Phys. Chem. A* **1997**, *101*, 9302. (e) Beagley, B.; Jones, M. O.; Houldsworth, N. *J. Mol. Struct.* **1980**, *62*, 105.

(36) (a) Guirgis, G. A. *J. Fluorine Chem.* **1984**, *25*, 405. (b) Tai, S.; Papasavva, S.; Kenny, J. E.; Gilbert, B. D.; Janni, J. A.; Steinfeld, J. I.; Taylor, J. D.; Weinstein, R. D. *Spectrochim. Acta Part A*, **1999**, *55*, 9.

(37) (a) Durig, J. R.; Liu, J.; Little, T. S.; Kalasinsky, V. A. *J. Phys. Chem.* **1992**, *96*, 8224. (b) Huber-Walchli, P.; Gunthard, Hs. *Spectrosc. Chim. Acta* **1981**, *37A*, 285.

(38) Scott, A. P.; Radom, L. *J. Phys. Chem.* **1996**, *100*, 16502.

(39) Pauling, L. *The Nature of the Chemical Bond*, 3rd ed.; Cornell University Press: Ithaca, NY, 1960.